Title: Balancing positive and negative selection: *in vivo* evolution of *Candida lusitaniae MRR1*

Running Title: Selection for and against constitutive Mrr1 activity

Elora G. Demers[a], Jason Stajich[b], Alix Ashare[c], Patricia Occhipinti[a], Deborah A. Hogan[a#]

[a]Department of Microbiology and Immunology, Geisel School of Medicine at Dartmouth, Hanover, New Hampshire, USA

[b]Department of Microbiology & Plant Pathology and Institute for Integrative Genome Biology, University of California-Riverside, Riverside, California, USA.

[c]Dartmouth-Hitchcock Medical Center, Section of Pulmonary and Critical Care Medicine, Lebanon, NH, USA

[#]Corresponding author:

Department of Microbiology and Immunology, Geisel School of Medicine at Dartmouth

Rm 208 Vail Building, Hanover, NH 03755

E-mail: deborah.a.hogan@dartmouth.edu

Tel: (603) 650-1252

Fax: (603) 650-1318

Keywords: *Candida lusitaniae,* Mrr1, evolution, drug resistance, fluconazole, yeast, hydrogen peroxide, chronic infection, cystic fibrosis, *Candida albicans*, *Candida auris*

Abstract

The evolution of pathogens in response to selective pressures present during chronic infections can influence persistence, virulence, and the outcomes of antimicrobial therapy. Because subpopulations within an infection can be spatially separated and the host environment can fluctuate, an appreciation of the pathways under selection may be most easily revealed through the analysis of numerous isolates from single infections. Here, we continued our analysis of a set of clonally-derived *Clavispora (Candida) lusitaniae* isolates from a single chronic lung infection with a striking enrichment in the number of alleles of *MRR1*. Genetic and genomic analyses found evidence for repeated acquisition of gain-of-function mutations that conferred constitutive Mrr1 activity. In the same population, there were multiple alleles with both gain-of-function mutations and secondary suppressor mutations that either attenuated or abolished the constitutive activity suggesting the presence of counteracting selective pressures. Our studies demonstrated tradeoffs between high Mrr1 activity, which confers resistance to the antifungal fluconazole, host factors, and bacterial products through its regulation of *MDR1*, and resistance to hydrogen peroxide, a reactive oxygen species produced in the neutrophilic environment associated with this infection. This inverse correlation between high Mrr1 activity and hydrogen peroxide resistance was observed in multiple *Candida* species and in serial analysis of populations from this individual collected over three years. These data lead us to propose that dynamic or variable selective pressures can be reflected in population genomics and that these dynamics can complicate the drug resistance profile of the population.

Importance

Understanding microbial evolution within patients is critical for managing chronic infections and understanding host-pathogen interactions. Here, our analysis of multiple *MRR1* alleles in isolates from a single *Clavispora (Candida) lusitaniae* infection revealed the selection for both high and low Mrr1 activity. Our studies reveal tradeoffs between high Mrr1 activity, which confers resistance to the commonly used antifungal fluconazole, host antimicrobial peptides and bacterial products, and resistance to hydrogen peroxide. This work suggests that spatial or temporal differences within chronic infections can support a large amount of dynamic and parallel evolution, and that Mrr1 activity is under both positive and negative selective pressure to balance different traits that are important for microbial survival.

Introduction

Understanding the positive and negative selective pressures that shape drug resistance profiles in microbial populations is critical for combating the development of antimicrobial resistance, an ever-increasing problem in clinical settings. Increased drug resistance in bacteria and fungi has been associated with clinically- and agriculturally-used antimicrobial agents (reviewed in (1-3)), and drug resistance elements may be selected for based on their ability to protect against factors produced by other microbes or plant, animal, and insect hosts (4, 5). Based on the analysis of bacterial isolates of *Burkholderia dolosa* or *Pseudomonas aeruginosa* from single patients and across cohorts of patients, it is clear that *in vivo* factors can lead to the repeated selection for subpopulations with the same genes or pathways mutated (6-8). Furthermore, there is evidence that pathways can be upregulated then downregulated in the same phylogenetic lineages. For example, suppressor mutations within *P. aeruginosa algU* frequently arise in strains with high AlgU signaling caused by mutations in the gene encoding the AlgU repressor MucA (9). Less is known about the negative selective pressures acting against sustained microbial resistance.

In Demers *et al*. (10), we described a set of twenty recently-diverged *Clavispora* (*Candida*) *lusitaniae* isolates obtained from the lung infection of a single individual with cystic fibrosis (CF). *C. lusitaniae* is among the emerging non-*albicans Candida* spp. that cause life threatening disseminated infections in individuals who are immunocompromised (11, 12), and can cause infections of the gastrointestinal tract (13-15), surgical sites, or implanted devices in immunocompetent individuals. *C. lusitaniae* is notorious for its rapid development of resistance to antifungal drugs including amphotericin B, azoles and echinocandins (14, 16-19) and, relative to *Candida albicans* and other *Candida* species that are both opportunistic pathogens and members of the mycobiome, it is more closely related to *Candida auris*, a species in which multi-drug

74 resistant isolates have caused hospital-associated outbreaks (20-26). Our previous analyses of
75 heterogeneity in fluconazole (FLZ) resistance among these isolates identified numerous distinct
76 alleles of *MRR1* (*CLUG_00542*). Multiple alleles encoded gain-of-function (GOF) mutations
77 causing constitutive Mrr1 activity, which, as in other *Candida* species, increased expression of
78 *MDR1* and Mdr1 multidrug efflux pump activity (10, 27-32). At the time that these isolates were
79 recovered, the patient had no history of antifungal treatment, suggesting that selection for
80 constitutively active Mrr1 variants may have been driven by the need for resistance to other host-
81 or microbe-produced compounds. Within this study, however, we found multiple lineages with
82 recently evolved *MRR1* alleles that rendered cells more sensitive to FLZ than even *mrr1*Δ strains.
83 Here, we address the perplexing question of why this population had recently diverged *MRR1*
84 alleles that encoded both high and low Mrr1 activity. To do so, we expressed both native and
85 synthesized *MRR1* alleles that represent intermediates during *MRR1* evolution in a common
86 genetic background and tested the effects of these alleles on growth in *in vivo* relevant conditions.
87 Using genetics and genomics, we concluded that multiple *C. lusitaniae MRR1* alleles that
88 conferred low Mrr1 activity resulted from initial mutation that caused constitutive Mrr1 activity
89 followed by a second mutation that either suppressed constitutive activation or inactivated the
90 protein. Constitutive Mrr1 activity caused increased sensitivity to a variety of biologically relevant
91 compounds including hydrogen peroxide (H_2O_2) and suppression of constitutive Mrr1 activity
92 rescued growth under many of these conditions. Monitoring populations from respiratory samples
93 from this subject over time supports the model that there are opposing selective pressures *in vivo*
94 that select for and against constitutive Mrr1 activity, as reflected by the tradeoff between FLZ and
95 H_2O_2 resistance seen over time. These data explain the persistence of a heterogeneous fungal

96 population and underscores the complexity and parallelism of evolution that is possible in the
97 human lung during chronic disease.

98

99 **Results**

100 **Naturally evolved *C. lusitaniae MRR1* alleles confer altered Mrr1 activity and FLZ resistance**

101 Each of the twenty closely-related *C. lusitaniae* isolates from a single individual contained
102 at least one nonsynonymous single nucleotide polymorphism (SNP) or single nucleotide insertion
103 or deletion (indel) in *MRR1* relative to the deduced *MRR1* sequence of their most recent common
104 ancestor ($MRR1^{ancestral}$) (Fig. 1A) (10). To determine the impact of specific mutations in *MRR1* on
105 Mrr1 activity, we expressed different *MRR1* alleles in a common genetic background in which the
106 native *MRR1* had been deleted (U04 *mrr1*Δ). Deletion of *MRR1* in the FLZ-resistant strain U04
107 reduced the FLZ minimum inhibitory concentration (MIC) from 32 μg/ml to 4 μg/ml (10) and the
108 decrease in MIC was complemented by restoring the native $MRR1^{Y813C}$ allele (Fig. 1B).
109 Complementation of U04 *mrr1*Δ with the $MRR1^{ancestral}$ allele led to a FLZ MIC of 1 μg/ml which
110 was 4-fold lower ($P<0.0001$) than the FLZ MIC of U04 *mrr1*Δ, suggesting that $MRR1^{ancestral}$ had a
111 function that reduced the FLZ MIC (Fig. 1B). Expression of an *MRR1* allele from a FLZ-sensitive
112 isolate in the population ($MRR1^{L1191H+Q1197*}$) also reduced the FLZ MIC to levels comparable to
113 those for $MRR1^{ancestral}$ (0.5-1 μg/ml) (Fig. 1B). Similar correlations between *MRR1* allele and FLZ
114 MIC were observed when the $MRR1^{ancestral}$, $MRR1^{Y813C}$, and $MRR1^{L1191H+Q1197*}$ alleles were expressed
115 in a *mrr1*Δ derivative of the FLZ-sensitive strain U05, which indicated that strain background did
116 not contribute to the FLZ MIC conferred by different *MRR1* alleles (Fig. 1C). We previously
117 published that FLZ resistance correlated with expression of *MDR1* (10), also referred to as *MFS7*

(19). Deletion of *MDR1* reduced the MIC, and the MIC was even lower in U04 *mrr1*Δ*mdr1*Δ (Fig. S1A) indicating that the moderately higher levels of FLZ resistance in U04 *mrr1*Δ compared to a strain with *MRR1*^{ancestral} was *MDR1*-dependent.

RNA-sequencing (RNA-seq) analysis validated the previously published result that *MDR1* correlated with the FLZ MIC for the different Mrr1 variants (10). The expression of *MGD1* and *MGD2*, two *C. lusitaniae* genes shown to be Mrr1-regulated, correlated with the expression of *MDR1* (Fig. 1D and Table S1) (10, 13, 33). Gene expression differences between U04 (*MRR1*^{Y813C}), U04 *mrr1*Δ, and U04 *mrr1*Δ +*MRR1*^{Y813C} found that *mrr1*Δ is fully complemented upon return of *MRR1*^{Y813C} to the native locus (Fig. 1D and Fig. S2A for correlation plot) and that Mrr1 positively and negative regulates a large set of genes. Furthermore, a correlation analysis found that U04 *mrr1*Δ +*MRR1*^{ancestral} and U04 *mrr1*Δ +*MRR1*$^{L1191H+Q1197*}$ were similar to each other but distinct from the *mrr1*Δ (Fig. S2A and 1B). A linear model comparing these strains identified forty-one genes with at least a 2-fold change in expression and corrected *P* value <0.05 (FDR). Comparison of non-isogenic *C. lusitaniae* strains similarly identified at least fourteen of the genes in Table S1 as putatively Mrr1-regulated (10, 13). Eighteen genes were homologs or had similar predicted functions as genes previously published as regulated by *C. albicans* Mrr1 (29), including *MDR1, FLU1* and multiple putative methylglyoxal reductases encoded by *GRP2*-like genes, such as *MGD1* and *MGD2* (Fig. 1D and Table S1). Other genes within the Mrr1 regulon are discussed further below.

The unexpected finding that FLZ MIC was higher upon deletion of *MRR1* relative to a strain with *MRR1*^{ancestral} or an allele from a FLZ-sensitive strain was also observed in distantly-related *C. lusitaniae* strains, ATCC 42720 and DH2383 (FLZ MICs of ~1-2 μg/ml). In both cases, deletion of *MRR1* led to a 2-4-fold increase in FLZ MIC to 4-8 μg/ml (Fig. S1B, *P*<0.001). The

increase in FLZ MIC in *mrr1*Δ strains was not due to introduction of the selectable marker, *NAT1*, which encodes a nourseothricin acetyltransferase (34), as expression of *NAT1* from an intergenic site in the FLZ-sensitive U05 strain did not increase the FLZ MIC (Fig. S1C). These data led us to hypothesize that some Mrr1 variants ($MRR1^{Y813C}$) lead to high Mdr1 activity while other Mrr1 variants (both $MRR1^{ancestral}$ and the recently-diverged $MRR1^{L1191H+Q1197*}$ alleles) repressed the expression of at least some Mrr1-controlled genes, such as *MDR1*. Indeed, the RNA-Seq analysis identified six genes, including *MDR1*, that while positively regulated when Mrr1 was constitutively active, were more highly expressed in U04 *mrr1*Δ than those strains encoding low activity Mrr1 variants (Fig. 1D and S2B). These data suggest that, for a small subset of Mrr1-regulated genes, including *MDR1*, low activity Mrr1 variants directly or indirectly inhibit gene expression.

Truncation of *MRR1* has varied effects on Mrr1 activity and inducibility in clinical isolates

All twenty sequenced clinical *C. lusitaniae* isolates from a single human subject (Fig. 1A) had *MRR1* alleles with either one or two nonsynonymous mutations relative to $MRR1^{ancestral}$, and we found that *C. lusitaniae* isolates with two mutations in *MRR1* had a significantly lower average FLZ MIC than isolates with a single *MRR1* mutation (Fig. 2A, $P<0.001$) (10). Interestingly, six of the seven *MRR1* alleles in the "two mutation" set encoded premature stop codons, resulting in loss of 34-906 amino acids (Fig. 2B). There were two instances in which the same mutation was found with different nonsense mutations (*) or single nucleotide indels that led to early termination (t): $MRR1^{\mathbf{Y1126N}+P1174P(t)}$ or $MRR1^{\mathbf{Y1126N}+S359*}$, and $MRR1^{\mathbf{R1066S}+K912N(t)}$, $MRR1^{\mathbf{R1066S}+Y1061*}$ or $MRR1^{\mathbf{R1066S}+G1231*}$ (common mutation in bold, Fig. 1A) suggesting a complex evolutionary history for these alleles.

To better understand the effects of *MRR1* mutations on Mrr1 activity, we analyzed the effects of a chemical inducer of Mrr1 activity, benomyl (35-37), on *MDR1* expression. Benomyl

strongly induced *MDR1* expression in an Mrr1-dependent manner in the FLZ-sensitive strain ATCC 42720 (Fig. 2C) and, to a lesser extent, in the FLZ-resistant strain U04, which has high basal *MDR1* expression (Fig. 2D) (10). Quantitative RT-PCR analysis of *MDR1* expression and induction by benomyl in this collection of clinical isolates with different Mrr1 variants found that the two isolates with the lowest basal *MDR1* expression and lowest FLZ MIC (U05 and U07) had the greatest induction by benomyl (34- and 27-fold, respectively) (Fig. 2D). Three isolates, L11, L12 and U06, had intermediate FLZ MICs and *MDR1* expression levels, and did not show benomyl induction, similar to *mrr1*Δ, and all encoded Mrr1 variants lacking greater than 200 amino acids leading us to propose that these mutations caused a loss of Mrr1 function (Fig. 2D). Other isolates showed a correlation between higher basal *MDR1* levels and elevated FLZ MICs, and this pattern was associated with lower relative levels of benomyl induction (Fig. 2D).

Premature stop codons repeatedly arose in constitutively active Mrr1 variants and caused either a loss of constitutive Mrr1 activity or complete loss of function

In light of the mixed effects that these two-mutation *MRR1* alleles had on Mrr1 activity, we sought to determine the individual effects of mutations within each allele with a focus on the two strains with the lowest basal *MDR1* expression and the strongest induction of *MDR1* in response to benomyl: $MRR1^{L1191H+Q1197*}$ (in U05) and $MRR1^{\mathbf{Y1126N}+P1174P(t)}$ (in U07) (Fig. 3A and 3B). We found that the $MRR1^{L1191H}$ mutation caused a 32-fold increase in FLZ MIC (Fig. 3C) and 22-fold increase in *MDR1* expression (Fig. 3D) compared to $MRR1^{ancestral}$ indicating that, like the Mrr1-Y813C variant, Mrr1-L1191H was constitutively active. In contrast, $MRR1^{Q1197*}$, which caused the loss of 68 amino acids from the C-terminus of Mrr1, did not significantly alter the FLZ MIC compared to $MRR1^{ancestral}$ allele indicating that it was neither a constitutively activating nor a null mutation (Fig. 3C). The reintroduction of the Q1197* mutation into $MRR1^{L1191H}$, yielding

187 *MRR1*$^{L1191H+Q1197*}$, resulted in a 128-fold decrease in FLZ MIC (Fig. 3C) and 38-fold lower *MDR1*
188 expression values (Fig. 3D) compared to a strain expressing *MRR1*^{L1191H} and led to a phenotype
189 that mirrored that of *MRR1*^{ancestral}. Benomyl inducibility of these variants is discussed below.

190 *MRR1*$^{\mathbf{Y1126N}+P1174P(t)}$ (from U07) and *MRR1*$^{\mathbf{Y1126N}+S359*}$ (from the closely-related U06, Fig. 1A),
191 were similarly analyzed (Fig. 3B). Expression of *MRR1*^{Y1126N} in U04 *mrr1*Δ created a strain with a
192 high FLZ MIC (32-64 μg/ml, Fig. 3C) and *MDR1* expression (Fig. 3D), similar to that for strains
193 with *MRR1*^{Y813C} or *MRR1*^{L1191H}. Addition of the frameshift-inducing indel at P1174, which causes
194 a premature stop codon at N1176 removing 89 amino acids, yielding *MRR1*$^{Y1126N+P1174P(t)}$, caused a
195 128-fold decrease in the FLZ MIC and >100-fold decrease in *MDR1* expression relative to the
196 strain expressing *MRR1*^{Y1126N} again leading to a strain that phenocopied that with *MRR1*^{ancestral} (Fig.
197 3C and 3D). The addition of the indel at P1174 into an allele with a different constitutively active
198 variant, Mrr1-Y813C, (*MRR1*$^{Y813C+P1174P(t)}$) also caused a 256- and >100-fold decrease in FLZ MIC
199 and *MDR1* expression, respectively, (Fig. 3C and 3D). In contrast, addition of a SNP causing an
200 early stop codon at S359 to the allele with the activating Y1126N mutation (*MRR1*$^{Y1126N+S359*}$)
201 yielded a strain that phenocopied U04 *mrr1*Δ, indicating this variant was inactive (Fig. 3C and
202 3D). Together, these data suggest that the Y1126N mutation caused constitutive Mrr1 activity, that
203 was subsequently suppressed by premature stop codons that either restored Mrr1 repression of
204 *MDR1* (P1174P(t)) or eliminated activity (S359*). The RNA-Seq analysis supported the results
205 that premature stop codons near the very end of the protein converted constitutively active variants
206 into ones that yielded expression profiles to those for *MRR1*^{ancestral} and that were distinct from
207 *mrr1*Δ (Fig. 1D).

208 In addition to the differences in basal activity, the individual mutations alone and in
209 combination affected chemical inducibility by benomyl. Levels of *MDR1* were strongly induced

by benomyl in U04 *mrr1*Δ+ *MRR1*^{ancestral} (40-fold increase), but not in the U04 parental strain with high Mrr1 activity or its *mrr1*Δderivative (Fig. 3D). Along with the native Mrr1-Y813C, two other constitutively active Mrr1 variants (Mrr1-L1191H and Mrr1-Y1126N) showed only a 2-3-fold increase in *MDR1* expression with benomyl (Fig. 3D) similar to what was observed for more FLZ resistant clinical isolates (Fig. 2D). Surprisingly, addition of the mutations that caused premature stop codons within the last 100 amino acids of Mrr1 to the constitutively active Mrr1-L1191H, Mrr1-Y1126N and Mrr1-Y813C variants restored inducibility by benomyl (Fig. 3D). In fact, there was a strong and significant inverse correlation between basal *MDR1* expression and fold induction by benomyl (Fig. 3E).

As in *C. albicans*, *C. lusitaniae* Mrr1 regulates the expression of the methylglyoxal reductase encoded by *MGD1* (*CLUG_01281* or *GRP2*) (10, 29, 33, 38) and the multidrug efflux pump encoded by *FLU1* (*CLUG_05825*) (10, 39, 40) (Table S1 and Fig. S3A). As with *MDR1*, expression of both *MGD1* and *FLU1* was significantly higher in strains encoding the constitutively active Mrr1-Y813C, Mrr1-Y1126N and Mrr1-L1191H variants, compared to a strain encoding the Mrr1-ancestral variant, and the absence of the C-terminus in strains with activating mutations caused a significant decrease in basal *MGD1* and *FLU1* expression (Fig. S3B and S3C). Benomyl induction of *MGD1*, like *MDR1* (Fig. S3D), was restored upon loss of the C-terminus of the constitutively active Mrr1 variants further supporting the strong negative correlation between basal expression and induction by benomyl (Fig. 2F and S3E). *FLU1* expression, however, was not induced by benomyl in any strain suggesting that *FLU1* regulation by Mrr1 differs from *MGD1* and *MDR1* (Fig. 2G and S3F). Interestingly, *MDR1* and *MGD1*, while highly differentially expressed depending on Mrr1 activity (~20-fold or greater), were both de-repressed in the absence of Mrr1, and *FLU1* was not and was only weakly differentially expressed (<2-fold) (Fig. 1D and

S2B). Together these data indicate the C-terminus of Mrr1 is required for constitutive expression of multiple Mrr1-regulated genes, but not for benomyl induction of the Mrr1-regulated genes tested (Fig. S3A). Combined with the Mrr1 activity across clinical isolates (Fig. 2D), these data indicate that in strains with constitutively active Mrr1 variants, there was selection for mutations to decrease Mrr1 activity, resulting in a mixed population containing constitutively active, truncated but inducible, and loss-of-function Mrr1 variants.

Constitutive Mrr1 activity negatively impacts H_2O_2 resistance

We next sought to understand why mutations that reduce Mrr1 activity might repeatedly arise in this chronic infection. Previous studies have shown that overexpression of drug efflux pumps in drug resistant microbes can cause a fitness defect due to the energetic cost of constitutive pump production and activity in the absence of a selective substrate (41-43). Deletion of *MDR1* from U04 *mrr1*Δ +*MRR1*^{Y813C}, which constitutively expresses *MDR1*, however, did not alter the growth rate across multiple carbon sources (Fig. 4A). In the absence of an obvious fitness defect, we considered factors present in the CF lung, which has been characterized as a highly inflamed environment containing an abundance of neutrophils and macrophages, and high oxidative stress (reviewed in (44, 45)). While little is known about the effects of fungus dominated chronic lung infections in CF, such as the infection from which these isolates originated, an analysis of cytokines within the bronchoalveolar lavage (BAL) fluid from the patient these isolates originated from showed pro-inflammatory cytokines (IL-8 and IL-1β) present were consistent with the neutrophilic environment seen in other patients with CF (Fig. 4B) (45).

In light of these findings, we investigated the effects of Mrr1 activity on reactive oxygen species (ROS) stress generated by hydrogen peroxide (H_2O_2), a stress strongly associated with high neutrophil counts. In a serial dilution assay, we found that isogenic strains encoding constitutively

active Mrr1 variants, while highly resistant to FLZ and diamide (Fig. S4A), had increased sensitivity to 4 mM H_2O_2 compared to those expressing the Mrr1-ancestral variant (Fig. 4C). Diamide was used to illustrate relative Mrr1 activity instead of FLZ because serial dilution assays on rich medium (YPD) containing FLZ are not always representative of FLZ MIC, which are assessed in defined medium (Fig. S4B). Resistance to H_2O_2 was restored by addition of mutations causing both mild and severe premature stop codons (Fig. 4C, S4A). The effects of Mrr1 activity on H_2O_2 sensitivity were independent of strain background, as similar results were seen in isogenic strains in the U04 and U05 backgrounds (Fig. 4C and S4B). Surprisingly, deletion of *MDR1* from a strain encoding the constitutively active Mrr1-Y813C variant partially rescued growth (Fig. 4C and S4A), however, the absence of *MDR1* did not completely explain the differences as strains lacking *MRR1* had increased H_2O_2 resistance despite elevated *MDR1* expression (Fig. 4C). Additionally, the double mutant U04 *mrr1*Δ *mdr1*Δ did not have increased resistance to H_2O_2 compared to U04 *mrr1*Δ (Fig. 4C), suggesting this may be a complex response. A secondary assay quantifying growth after ~24 hours in liquid cultures containing 1 mM H_2O_2, though variable day-to-day, confirmed there was a reproducible difference in growth between strains encoding the low activity Mrr1-ancestral and constitutively active Mrr1-Y813C variants (Fig. 4D). Consistent with the plate-based assay, the absence of *MDR1* appeared to account for some but not all of the differences in growth in H_2O_2 (Fig. 4D). To determine if this phenomenon was unique to *C. lusitaniae* Mrr1 we examined a set of isogenic *C. albicans* isolates (40), and *in vivo* or *in vitro* evolved *C. dubliniensis* isolates (30) expressing *MRR1* alleles containing GOF mutations. We found that for all *C. albicans* and *C. dubliniensis* strain sets tested, strains with high Mrr1 activity, which were more resistant to FLZ (40, 46, 47) and diamide, were more sensitive to H_2O_2 than

278 strains with low Mrr1 activity or lacking *MRR1* (Fig. 4C). These data show that the Mrr1 activity
279 driven tradeoff between FLZ and H_2O_2 resistance is conserved across multiple *Candida* species.

280 A screen of isogenic strains for growth in varying concentrations of 48 chemical
281 compounds resuspended from the Biolog Phenotype MicroArrays MicroPlates (Fig. S5) supported
282 our findings that constitutive Mrr1 activity can increase sensitivity to oxidative stress. When
283 comparing strains encoding either the low activity Mrr1-ancestral variant or the constitutively
284 active Mrr1-Y813C variant, with either *MDR1* intact or removed, we found there were no
285 differences in growth in the medium used to resuspend the Biolog compounds (Fig. S5A) and
286 many conditions caused less than a 25% difference in growth (Fig. S5B). Unsurprisingly,
287 constitutive Mrr1 activity conferred Mdr1-dependent resistance to twelve compounds, including
288 three triazoles (FLZ, propiconazole, myclobutanil) (Fig. S5B and S5C). High Mrr1 activity also
289 led to Mdr1-independent resistance to four additional compounds, including two other azoles (3-
290 amino-1, 2, 4-triazole and miconazole nitrate) (Fig. S5B and S5C). Eight compounds caused a
291 largely Mdr1-independent decrease in growth in strains encoding the constitutively active Mrr1-
292 Y813C variant: 6-azauracil, berberine, BAPTA, lithium chloride, aminacrine, sodium metasilicate,
293 pentamidine isethionate and potassium chromate (Fig. S5D). Interestingly, berberine and azaserine
294 have previously been studied for their toxic effects on FLZ-resistant *Candida* strains (48, 49) and
295 calcium inhibitors, such as BAPTA, have been reported to interfere with antifungal resistance (50,
296 51). While diverse, these compounds are broadly reported to effect metabolism and respiration
297 (52-56), which can lead to oxidative damage via the production of ROS, and/or DNA/RNA
298 integrity, either by direct binding or oxidative damage (57-62). Strain lacking *MRR1* or encoding
299 a functional Mrr1 variant that contains a premature stop codon (<100 amino acids removed) were

not sensitive to most of these compounds, suggesting secondary mutations causing a decrease or loss of Mrr1 activity could restore resistance in some environments (Fig. S5D).

To gain insight into the mechanisms that lead to differences in oxidative stress resistance between strains with different levels of Mrr1 activity, we compared the gene expression profiles after a 30-minute exposure to 0.5 mM H_2O_2, a partially inhibitory concentration. H_2O_2 exposure had broad strain-independent effects on the transcriptome, altering expression of 786 genes (FC≥2, FR<0.05) including increased expression of *CLUG_04072*, a homolog of *C. albicans CAT1*, which was previously shown to be important for the resistance of *C. lusitaniae* to H_2O_2 (63) (Fig. S6A and Table S2). While there were subtle differences in the H_2O_2 response between strains expressing the constitutively active Mrr1-Y813C variant compared to U04 *mrr1*Δ *MRR1*^{ancestral} there were no clear patterns that would explain the difference in H_2O_2 resistance (Fig. S6B). The majority of differences in gene expression were seen in the magnitude of induction of Mrr1-regulated genes by H_2O_2, a known inducer of Mrr1 in other species (29, 64), indicating that, as with benomyl (Fig. S3D-F), strains with constitutively active Mrr1variants are less inducible than strains with low activity variants (Fig. S6B and S6C). Next, we investigated the expression of homologs of oxidative stress response (OSR) genes previously characterized in *C. albicans* and *S. cerevisiae* and found that there was not a significant Mrr1-dependent difference in basal or H_2O_2-induced expression of these genes (Fig. S6A). Genes assessed included the oxidative stress responsive transcription factor encoded by *CaCAP1* or *ScYAP1*, superoxide dismutase (*SOD2, SOD4, SOD6*), enzymes involved in the thioredoxin (*TSA1, TRX1, TRR1*) and glutathione (*GPX, GSH1*) systems, catalase (*CAT1*), and OSR genes involved in carbohydrate metabolism and the DNA-damage response (65, 66). Further analysis is required to better understand the link between constitutive Mrr1 activity and H_2O_2 sensitivity, however these data highlight that the sensitivity is not due to

failure to induce an oxidative stress response, but more-likely a consequence of the activity of Mrr1-regulated genes, such as *MDR1* (Fig. S4A and S4C).

Phenotype dynamics in chronic infection populations over time

In light of the evidence for complex evolution of *MRR1* and the potentially advantageous phenotypes associated with both high and low Mrr1 activity, we sought to better understand the fractions of isolates with these Mrr1 associated traits over time. For this analysis, we used arrayed *C. lusitaniae* populations isolated from sputum or one BAL procedure collected from the same subject over three years, with the first time point approximately six months after the first clinical culture report of the high levels of "non-*albicans Candida*" (NAC) as shown in Fig. 5A. Upon plating isolates on agar with FLZ (8 μg/ml) or H_2O_2 (4 mM) (Fig. 5A), we found an inverse correlation between robust growth on FLZ and robust growth on H_2O_2. It was uncommon for isolates to be inhibited or uninhibited in both conditions (Fig. S5A). Isolates from the early samples were predominately sensitive to FLZ (10), but were largely resistant to H_2O_2. During and soon after the course of FLZ therapy (Sp1.5 and Sp2, respectively), however, there was an increase isolates that were more FLZ resistant but H_2O_2-sensitive (Fig. 5A). Subsequent samples from two years after the FLZ therapy was completed varied in the proportion of isolates that grew better on H_2O_2 and FLZ. Thus, the *C. lusitaniae* population shifted back and forth between being dominated by isolates with higher H_2O_2 resistance or higher FLZ resistance, but both phenotypes remained in the population over time (Fig. 5B).

Discussion

A population of *C. lusitaniae* isolates first described in Demers *et al.* (10) contained an unexpectedly large number of nonsynonymous mutations in the gene encoding the transcription factor, Mrr1, which regulated FLZ resistance, suggesting that Mrr1 activity was under strong

346 selective pressure *in vivo*. These *MRR1* alleles contained either one or two nonsynonymous SNPs
347 or indels (Fig. 1A) and isolates with one mutation had on average higher FLZ resistance than those
348 with two nonsynonymous *MRR1* mutations (Fig. 2A). While multiple studies have shown that
349 constitutive Mrr1 activity is beneficial under multiple biologically relevant conditions, including
350 exposure to azoles (10, 29), bacterial-produced toxins including phenazines (10), and host-
351 produced antifungal peptides including histatin 5 (10, 40), it was unclear why *MRR1* alleles
352 conferring low Mrr1 activity would be selected for in this population (10). Deconstruction of
353 *MRR1* alleles with two mutations revealed an evolutionary path on which an activating mutation
354 arose first, followed by suppressing mutations that either restored low basal activity but retained
355 inducibility, or abolished Mrr1 activity altogether (Fig. 3 and S3). Interestingly, a *C. parapsilosis*
356 strain was recently found to contain a central domain mutation and a C-terminal truncation
357 ($Mrr1^{P295L+Q1074*}$) similar to the alleles described above, however, it is not currently known how
358 these mutation impact Mrr1 activity and FLZ resistance (67), suggesting that selection for and
359 against elevated Mrr1 activity may also occur in other *Candida* species.

360 Surprisingly, the RNA-Seq analysis of isogenic strains expressing different *MRR1* alleles
361 revealed that *C. lusitaniae* Mrr1 appears to positively and negatively regulate genes expression
362 (Fig. 1D) although further analysis is required to determine which genes are direct targets of Mrr1.
363 Adding to previous studies in *C. lusitaniae* (10, 13) and *C. albicans* (29), we found that Mrr1
364 positively regulates 41 genes with a fold change ≥ 2 and 102 genes with a fold change ≥ 1.5
365 (FDR<0.05). Mrr1-induced genes include multiple MFS and ABC transporters (*i.e. MDR1, FLU1,*
366 *CDR1*), methylglyoxal reductases (33), putative alcohol dehydrogenases, and a variety of other
367 putative metabolic genes (Table S1). Constitutively active Mrr1 also appears to repress expression
368 of 42 genes (fold change ≥ 1.5, FDR<0.05), including multiple iron and/or copper transporters and

369 reductases, and sugar transporters (Table S1). These data combined with Bierman *et al*., which
370 showed that *C. lusitaniae* Mrr1 is induced by the spontaneously formed stress signal methylglyoxal
371 (33), imply that Mrr1 may play a larger role in a generalized metabolic or stress response, beyond
372 what has been previously studied in response to FLZ and xenobiotic stressors.

373 While the C-terminal region of *C. lusitaniae* Mrr1 was necessary for constitutive Mrr1
374 activity, it was not required for induction of Mrr1-regulated genes, including *MDR1* and *MGD1*,
375 in response to benomyl (Fig. 2D, 3 and S3). Subsequent addition of mutations resulting in the loss
376 >200 amino acids, however, caused a slight decrease in FLZ resistance and *MDR1* expression, but
377 these variants were no longer inducible by benomyl and phenocopied strains completely lacking
378 *MRR1* (Fig. S1B, 3C and 3D). These data are consistent with previous studies showing C-terminal
379 truncations prior to amino acid 944 in *C. albicans MRR1*, homologous to position 1116 in *C.*
380 *lusitaniae MRR1*, caused a complete loss of CaMrr1 activity (68). The L11, L12 and U06 strains
381 encoding Mrr1 variants with premature stop codons before amino acid 1116 similarly phenocopied
382 *mrr1*Δ strains (Fig. 2C and 2D). Surprisingly, loss-of-function Mrr1 variants and *mrr1*Δ strains
383 had intermediate expression of a subset of the most strongly differentially regulated genes
384 compared to strains with low activity Mrr1 (Fig. S2B), which has not been observed in other
385 *Candida* species (29, 31, 32). Additional studies are required to determine if this phenomenon is
386 unique to *C. lusitaniae* or more broadly shared among non-*albicans Candida* species closely
387 related to *C. lusitaniae*, such as *C. auris* (20, 26), and if any of the co-regulators of the Mrr1
388 regulon described in *C. albicans* (64, 69, 70) are involved. These findings raised the question as
389 to why, if constitutive Mrr1 was initially selected for, would it later be selected against *in vivo*,
390 especially in the absence of an obvious growth defect (Fig. 4A and S5A).

Chronic lung infections are typically an inflamed environment (Fig. 4B) containing a high number of polymorphonuclear leukocytes (PMNs) that produce proteases, myeloperoxidases and ROS (71, 72), which is an important component of the immune system used to kill fungi (reviewed in (73)). In a screen of diverse chemical compounds, we found that strains with constitutive Mrr1 activity were more strongly inhibited by multiple compounds that have previously been shown to cause damage through oxidative stress (Fig. S5B-D). When we specifically interrogated H_2O_2 resistance, we found that *C. lusitaniae* strains encoding constitutively active Mrr1 variants were more sensitive than strain encoding low activity Mrr1 variants or lacking a functional Mrr1 (Fig. 4A, S4). Sensitivity to H_2O_2 and the compounds from the Biolog plates was at least partially dependent on Mdr1, thought other Mrr1-regulated genes may still contribute to the decreased growth under conditions of oxidative stress (Fig. S4B, S5 and S6). Interestingly, the tradeoff between FLZ and H_2O_2 resistance was conserved broadly among a time series of *C. lusitaniae* isolates and other *Candida* species (Fig. 4C and 5A).

As outlined in the model in Figure 5B, together these data highlight that changing environments within complex and dynamic chronic infections could contribute to the development of heterogeneous fungal populations. Though it appears that initial selection on the ancestral version of Mrr1 was driven by the need for increased Mrr1 activity, over time either these selective pressures were removed, or other pressures became dominant, resulting in a secondary wave of mutations. This secondary wave of mutations caused a decrease or loss of Mrr1 activity, which uniquely to *C. lusitaniae* further contributed towards a population with mixed levels of FLZ resistance (Fig. 5B). Though the exact selective pressures at play in this instance are unknown, these data highlight the importance of understanding how microbes evolve *in vivo*, as complex

413 environments, even in the absence of clinically used antifungals, can shape the microbial
414 population and lead to antimicrobial resistance.
415
416 **Materials and Methods**
417 **Strains and growth conditions**
418 *Candida* strains used in this study are listed in Table S3. All strains were stored as frozen
419 stocks with 25% glycerol at -80 ºC and subcultured on YPD (1% yeast extract, 2% peptone, 2%
420 glucose, 1.5% agar) plates at 30 ºC. Strains were regularly grown in YPD liquid medium at 30 ºC
421 on a roller drum. Cells were grown in YNB (0.67% yeast nitrogen base medium with ammonium
422 sulfate (RPI Corp)) liquid supplemented with either 2% glucose, 2% glycerol or 2% casamino
423 acids and in RPMI-1640 (Sigma, containing L-glutamine, 165 mM MOPS, 2% glucose) liquid as
424 noted. Media was supplemented with 8 μg/ml FLZ (stock 4 mg/ml in DMSO), 1 mM diamide
425 (stock 58 mM in water) or 1-6 mM H_2O_2 (30% w/v in water, ~9.8M) as noted. *Escherichia coli*
426 strains were grown in LB with either 100 μg/ml carbenicillin or 15 μg/ml gentamycin as necessary
427 to obtain plasmids. BAL fluid and sputum were obtained in accordance with institutional review
428 board protocols as described in (74).
429 **DNA for gene knockout constructs**
430 Gene replacement constructs for knocking out *MRR1* (*CLUG_00542*, as annotated in (10))
431 and *MDR1* (*CLUG_01938/9* (10)) were generated by fusion PCR as described in Grahl *et al*. (63).
432 All primers (IDT) used are listed in Table S4. Briefly, 0.5 to 1.0 kb of the 5' and 3' regions flanking
433 the gene was amplified from U04 DNA, isolated using the MasterPure Yeast DNA Purification
434 Kit (epiCentre). The nourseothricin (*NAT1*) or hygromycin (*HygB*) resistance cassette was
435 amplified from plasmids pNAT (75) and pYM70 (76), respectively, using the Zyppy Plasmid

436 Miniprep kit (Zymo Research). Nested primers within the amplified flanking regions were used to
437 stitch the flanks and resistance cassette together. PCR products for transformation were purified
438 and concentrated with the Zymo DNA Clean & Concentrator kit (Zymo Research) with a final
439 elution in molecular biology grade water (Corning).

440 **DNA for insertion of *NAT1* at neutral site in *C. lusitaniae* genome**

441 The approximately 4000 bp genomic region between *CLUG_03302* and *CLUG*_03303 on
442 chromosome 4, which was not predicted to contain any genes or promoter regions, was targeted
443 as a potentially neutral insertions site. To create plasmid DH3261 containing *NAT1* flanked by
444 homology to this region of chromosome 4, approximately 1.0 kb of the flanking regions (positions
445 228,652 – 229,651 and 229,701 – 230,691) were amplified from U05 gDNA. All primers (IDT)
446 used are listed in Table S4. *NAT1*was amplified from pNAT (75). PCR products were purified and
447 concentrated then assembled with the vector (pRS426 (77) linearized with KpnI-HF and SalI-HF
448 (New England BioLabs) and treated with the phosphatase rSAP (New England BioLabs)) using
449 the NEBuilder HiFi DNA Assembly cloning kit (New England BioLabs). Assemblies were
450 transformed into High Efficiency NEB®5-alpha competent *E. coli* (New England BioLabs). The
451 *NAT1* insertion construct was isolated from DH3261 by digestion with KpnI-HF and SalI-HF (New
452 England BioLabs).

453 **Plasmids for complementation of *MRR1***

454 Plasmids for complementing *MRR1* were created as described in Biermann *et al*, 2020 (33).
455 For naturally occurring *MRR1* alleles, we amplified i) the *MRR1* gene and terminator with ~1150
456 bp upstream for homology from the appropriate strain's genomic DNA, ii) the selective marker,
457 *HygB* from pYM70 (76), and iii) ~950 bp downstream of *MRR1* for homology from genomic U05
458 (identical sequence for all relevant strains) using primers (IDT) listed in Table S4. PCR products

459 were cleaned up using the Zymo DNA Clean & Concentrator kit (Zymo Research) and assembled
460 using the *S. cerevisiae* recombination technique previously described (78). Plasmids created in *S.*
461 *cerevisiae* were isolated using a yeast plasmid miniprep kit (Zymo Research) and transformed into
462 High Efficiency NEB®5-alpha competent *E. coli* (New England BioLabs). *E. coli* containing
463 pMQ30 derived plasmids were selected for on LB containing 15 μg/ml gentamycin. Plasmids from
464 *E. coli* were isolated using a Zyppy Plasmid Miniprep kit (Zymo Research) and subsequently
465 verified by Sanger sequencing with the Dartmouth College Genomics and Molecular Biology
466 Shared Resources Core. *MRR1* complementation plasmids were linearized with Not1-HF (New
467 England BioLabs), cleaned up the Zymo DNA Clean & Concentrator kit (Zymo Research) and
468 eluted in molecular biology grade water (Corning) before transformation of 2 μg into *C. lusitaniae*
469 strain U04 *mrr1*Δ as described below.

470 The $MRR1^{ancestral}$ allele sequence was amplified from gDNA of a closely related *C.*
471 *lusitaniae* isolate that had the same *MRR1* sequence but lacked any of the nonsynonymous
472 mutation that varied among the population of *C. lusitaniae* isolates described here. This *MRR1*
473 sequences does contain multiple synonymous and nonsynonymous mutations in comparison with
474 that of the reference strains, ATCC 42720 (79). Additional *MRR1* alleles were amplified from
475 gDNA from U04 ($MRR1^{Y813C}$), U05 ($MRR1^{L1191H+Q1197*}$), U02 ($MRR^{Y1126N+P1174P(t)}$) and U06
476 ($MRR1^{S359*+Y1126N}$). While making the pMQ30$^{MRR1\text{-}S359*+Y1126N}$ plasmid, one clone was identified that
477 lacked the S359* mutation resulting in the pMQ30$^{MRR1\text{-}Y1126N}$ plasmid. To create additional *MRR1*
478 alleles that were not identified within any *C. lusitaniae* isolates, pieces of *MRR1* were selectively
479 removed and repaired with DNA either containing or lacking the desired mutation. Because the
480 L1191H and Q1197* mutations were so close together, an alternate strategy was used to separate
481 these mutations from the $MRR1^{L1191H+Q1197*}$ allele. DNA fragments synthesized by IDT containing

either the L1191H or Q1197* mutations alone (sequences in Table S4) were amplified then assembled with pMQ30$^{MRR1\text{-}L1191H+Q1197*}$ (linearized with PvuI-HF) using the NEBuilder HiFi DNA Assembly cloning kit (New England BioLabs). To remove an unexpected nonsynonymous mutation in pMQ30$^{MRR1\text{-}Q1197*}$, this plasmid was digesting with EcoNI and repaired with a piece of DNA amplified from U04 *mrr1*Δ+*MRR1*^{ancestral} lacking the unwanted mutation. pMQ30^{MRR1} complementation plasmids was digested with Not1-HF (New England BioLabs) for transformation.

Strain construction

Mutants were constructed as previously described in Grahl *et al*. using an expression free ribonucleoprotein CRISPR-Cas9 method (63). 1 to 2 μg of DNA for gene knockout constructs generated by PCR or 2 μg of digested plasmid, purified and concentrated with a final elution in molecular biology grade water (Corning), was used per transformation. Plasmids containing complementation and knockout constructs and resulting strains are listed in Table S3 and crRNAs (IDT) are listed in Table S4. Transformants were selected on YPD agar containing 200 μg/mL nourseothricin or 600 μg/mL hygromycin B.

Drug susceptibility assays

Minimum inhibitory concentration (MIC) was determined using a broth microdilution method as previously described (80) with slight modifications (10). Briefly, $2x10^3$ cells were added to a two-fold dilution series of FLZ prepared in RPMI-1640, starting at an initial concentration of 64 μg/ml, then incubated at 35 ºC for 24 hours. The MIC was defined as the drug concentration that abolished visible growth compared to a drug-free control.

Quantitative RT-PCR

Overnight cultures were back diluted to an OD_{600} of ~0.1 and grown for 6 hours in YPD

liquid medium at 30°C. 50 μg/ml of benomyl (stock 10 mg/ml in DMSO) or an equivalent volume of DMSO were added for experiments assessing the induction of Mrr1 activity. 7.5 µg RNA (harvested using the MasterPure Yeast RNA Purification Kit (Epicentre)) was DNAse treated with the Turbo DNA-free Kit (Invitrogen). cDNA was synthesized from 300-500 ng of DNAse-treated RNA using the RevertAid H Minus First Strand cDNA Synthesis Kit (Thermo Scientific), following the manufacturer's instructions for random hexamer primer (IDT) and GC rich template. qRT-PCR was performed on a CFX96 Real-Time System (Bio-Rad), using SsoFast Evergreen Supermix (Bio-Rad) with the primers listed in Table S4. Thermocycler conditions were as follows: 95 ºC for 30 s, 40 cycles of 95 ºC for 5 s, 65 ºC for 3 s and 95 ºC for 5 s. Transcripts were normalized to *ACT1* expression.

RNA Sequencing

Overnight cultures were back diluted into YPD and grown to exponential (~8 h) twice, then treated with vehicle or 0.5 mM H_2O_2 for 30 minutes, in biological triplicate. RNA was harvested from snap-frozen pellets (using liquid nitrogen) using the MasterPure Yeast RNA Purification Kit (Epicentre) and stored at -80 ºC. RNA libraries were prepared using the Kapa mRNA HyperPrep kit (Roche) and sequenced using single-end 75 bp reads on the Illumina NextSeq500 platform. The data analysis pipeline is available in github repository (https://github.com/stajichlab/RNASeq_Clusitaniae_MRR1) and archived as DOI: [To be generated]. FASTQ files were aligned to the ATCC 42720 (79) genome with the splice-site aware and SNP tolerant short read aligner GSNAP (v v2019-09-12) (81). The alignments were converted to sorted BAM files with Picard (v2.18.3; https://broadinstitute.github.io/picard/) and read counts computed with featureCounts (v1.6.2) (82) with updated genome annotation to correct truncated gene model for locus *CLUG_00542*, and combine a single gene split into two,

528 *CLUG_01938_1939*; reasoning for these changes explained in (10). Differential gene expression
529 analyses were performed with the edgeR (83) package in Bioconductor, by fitting a negative
530 binomial linear model. The resulting *P* values were corrected for multiple testing with Benjamini-
531 Hochberg to control the false discovery rate. Genes for which there were less than 2 counts per
532 million (CPM) across the three (absent genes) were not included for differentially expressed gene
533 analysis. Two separate linear models were created to define the Mrr1 regulon in control conditions
534 alone and determine the interaction between Mrr1 activity and H_2O_2 exposure.

535 To define the Mrr1 regulon in YPD alone we identified genes differentially expressed
536 between strains with constitutive Mrr1 activity (U04 and U04 *mrr1*Δ +*MRR1*^{Y813C}) and low Mrr1
537 activity (U04 *mrr1*Δ, U04 *mrr1*Δ +*MRR1*^{ancestral}, and U04 *mrr1*Δ +*MRR1*$^{L1191H+Q1197*}$); this model
538 contained 5,474 genes. We discarded genes for which i) the $\log_2$FC greater than 1 (2-fold, see Fig.
539 1B) or 0.585 (1.5-fold, see Table S1) with an FDR<0.05, (ii) the average CPMs for replicates was
540 not greater than 10 for any strain, and ii) expression in both U04 and U04 *mrr1*Δ +*MRR1*^{Y813C} was
541 similar. Results are summarized in Table S1, including the Mrr1 regulon (Table S1a), and the
542 normalized CPMs/gene used for this linear model(Table S1b).

543 To determine how constitutive Mrr1 activity impacted the response to H_2O_2 we identified
544 the overlap between the interaction between U04 or U04 *mrr1*Δ +*MRR1*^{Y813C} and exposure to 0.5
545 mM H_2O_2, as compared to the reference strain (U04 *mrr1*Δ +*MRR1*^{ancestral}) and condition (YPD
546 alone); this model contained 5600 genes. Results are summarized in Table S2, including the
547 interaction between strains with constitutively active Mrr1 and H_2O_2 (Table S2a), the effect of
548 H_2O_2 treatment (Table S2b), and all normalized CPMs/gene used for this linear model (Table S2c).

549 **Biolog Phenotype MicroArrays analysis**

550 For the chemical sensitivity screen, the chemicals in Biolog plates PM22D and PM24C

were resuspended in 100 ul YPD liquid and transferred to a sterile 96-well polystyrene plate (Fisher) for kinetic measurements. 100 ul of cells adjusted to an OD of 0.01 in YPD was added to each well. Plates were incubated at 37 ºC for 24 hours. A control plate containing no drug was grown simultaneously for comparison.

Serial dilution assays

Following growth in YPD medium overnight with aeration at 30°C, cultures were diluted in water to an OD_{600} of 1. Serial dilutions of ten-fold were carried out in a microtiter plate to yield six concentrations ranging from approximately 10^7 cells/ml (for OD_{600} of 1) to approximately 10^2 cells/ml. 5 µl of each dilution were applied to YPD plates containing 4 or 5 mM H_2O_2 (stock 30% w/v, 9.8 M) or 1 mM diamide (stock 58 mM in water). Images were captured after incubation at 37°C for 24 or 48 hours.

Luminex Analysis

Cytokines in BAL fluid samples were measured (pg/ml) in singlicate by Luminex using a Millipore human cytokine multiplex kits (EMD Millipore Corporation, Billerica, MA) according to manufactures instructions. Assays were performed by the DartLab – Immune Monitoring and Flow Cytometry Resource core at Dartmouth.

Statistical analyses

Statistical analyses were done using GraphPad Prism 6 (GraphPad Software). Unpaired Student's t-tests (two-tailed) with Welch's correction were used to evaluate the difference in FLZ MIC between isolates containing one of two mutations in *MRR1*. One and two-way ANOVA tests were performed across multiple samples with either Tukey's multiple comparison test for unpaired analyses or Sidak's multiple comparison test for paired analyses conducted in a pairwise fashion.

573 *P* values <0.05 were considered as significant for all analyses performed and are indicated with
574 asterisks: **P*<0.05, ***P*<0.01, ****P*<0.001 and *****P*<0.0001.

575 **Data availability**

576 The data supporting the findings in this study are available within the paper and its
577 supplemental information and are also available from the corresponding author upon request. The
578 raw sequence reads from the RNA-Seq analysis have been deposited into NCBI sequence read
579 archive under BioProject PRJNA680763. Raw and processed RNA-Seq count data are available
580 in Gene Expression Omnibus (GSE162151) and include minor updates to the genome annotation
581 and assembly for *C. lusitaniae*.

582

583 **Figures and figure legends**

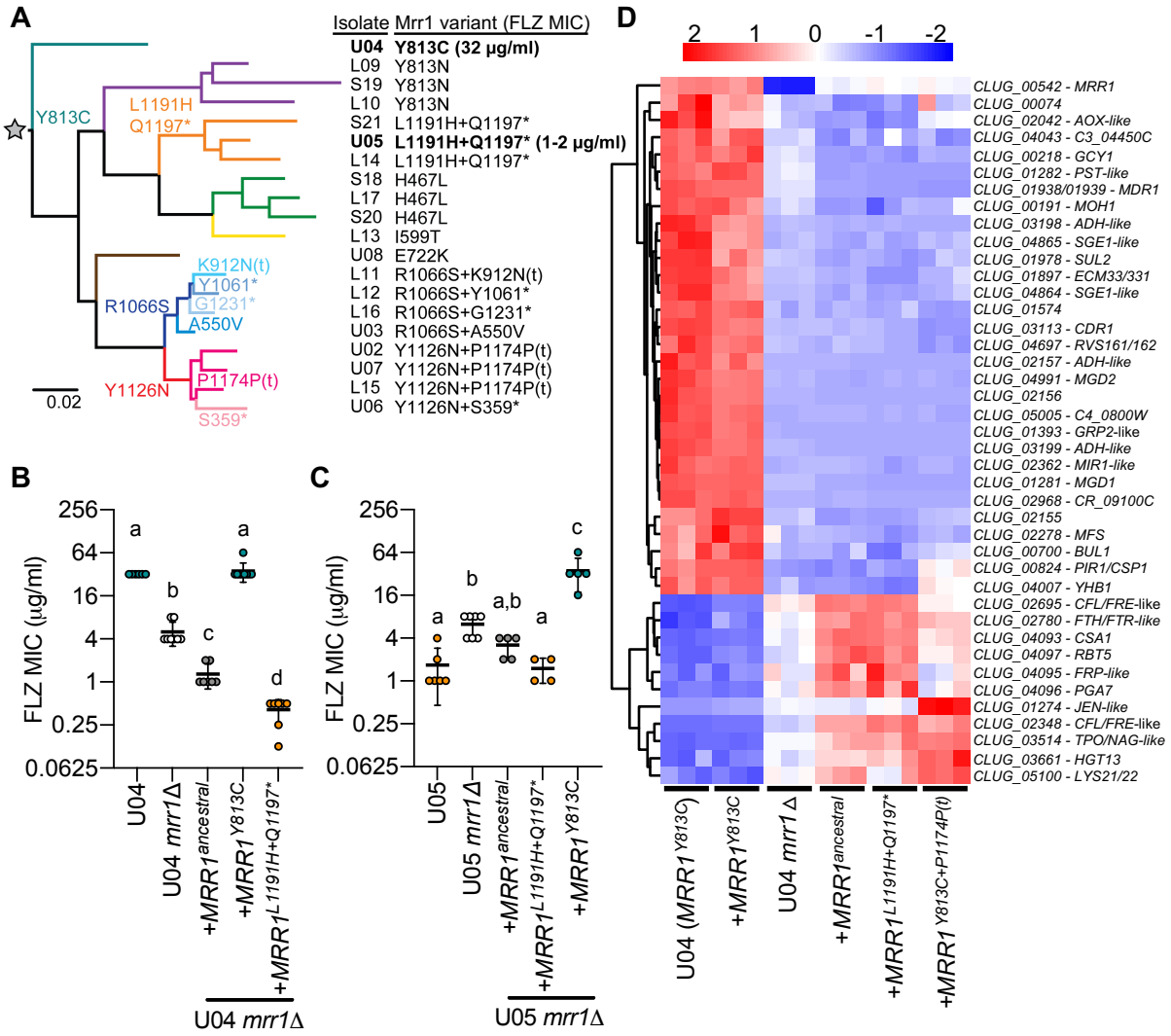

584

585 **Fig. 1: Naturally-evolved *MRR1* alleles confer higher or lower FLZ resistance compared to**
586 **strains expressing the ancestral *MRR1* allele. A**, Maximum likelihood-based phylogeny based
587 on whole genome sequences of twenty previously sequenced *C. lusitaniae* isolates, modified from
588 Demers, *et al*. (10). Select branchpoints are marked with the Mrr1 variants present in subsequent
589 isolates. Mrr1 variants are identified by amino acid changes that resulted from SNPs or indels; *
590 indicates a stop codon. The one nucleotide indel in codons P1174 (insertion) and K912 (deletion)
591 cause frameshift mutations that resulted in early termination, denoted with 't', at N1176 and L927,

592 respectively. Gray star at the root of the tree denotes the 'ancestral' *MRR1* sequence, which lacks
593 any of the mutations listed. **B**, FLZ MIC for unaltered, *mrr1*Δ or *MRR1* complemented strains in
594 the FLZ-resistant U04 (native allele $MRR1^{Y813C}$) strain background. **C**, Same as in **B**, but in the
595 FLZ-sensitive U05 strain background (native allele $MRR1^{L1191H+Q1197*}$). Strains containing the same
596 *MRR1* allele in **B** and **C** are represented by circles of the same color. Data shown represents at
597 least four independent assays on different days. One-way ANOVA with Tukey's multiple
598 comparisons test of $\log_2$ transformed values for **B**: all pairwise comparisons, $P<0.0001$ and **C**: all
599 pairwise comparisons, $P<0.001$. **D**, Heatmap of normalized counts per million (CPM) from RNA-
600 Seq analysis for genes that were differentially regulated between both strains expressing $MRR1^{Y813C}$
601 (U04 and U04 *mrr1Δ* + $MRR1^{Y813C}$) and U04 *mrr1*Δ + $MRR1^{ancestral}$, U04 *mrr1*Δ +
602 $MRR1^{L1191H+Q1197*}$, and U04 *mrr1*Δ when grown in liquid YPD medium. Complemented strains are
603 denoted as by their respective *MRR1* alleles. Hierarchical clustering of row (genes) by Euclidean
604 distance, cutoffs used were FDR <0.05 and fold change ≥2; additional information available in
605 Table S1.
606

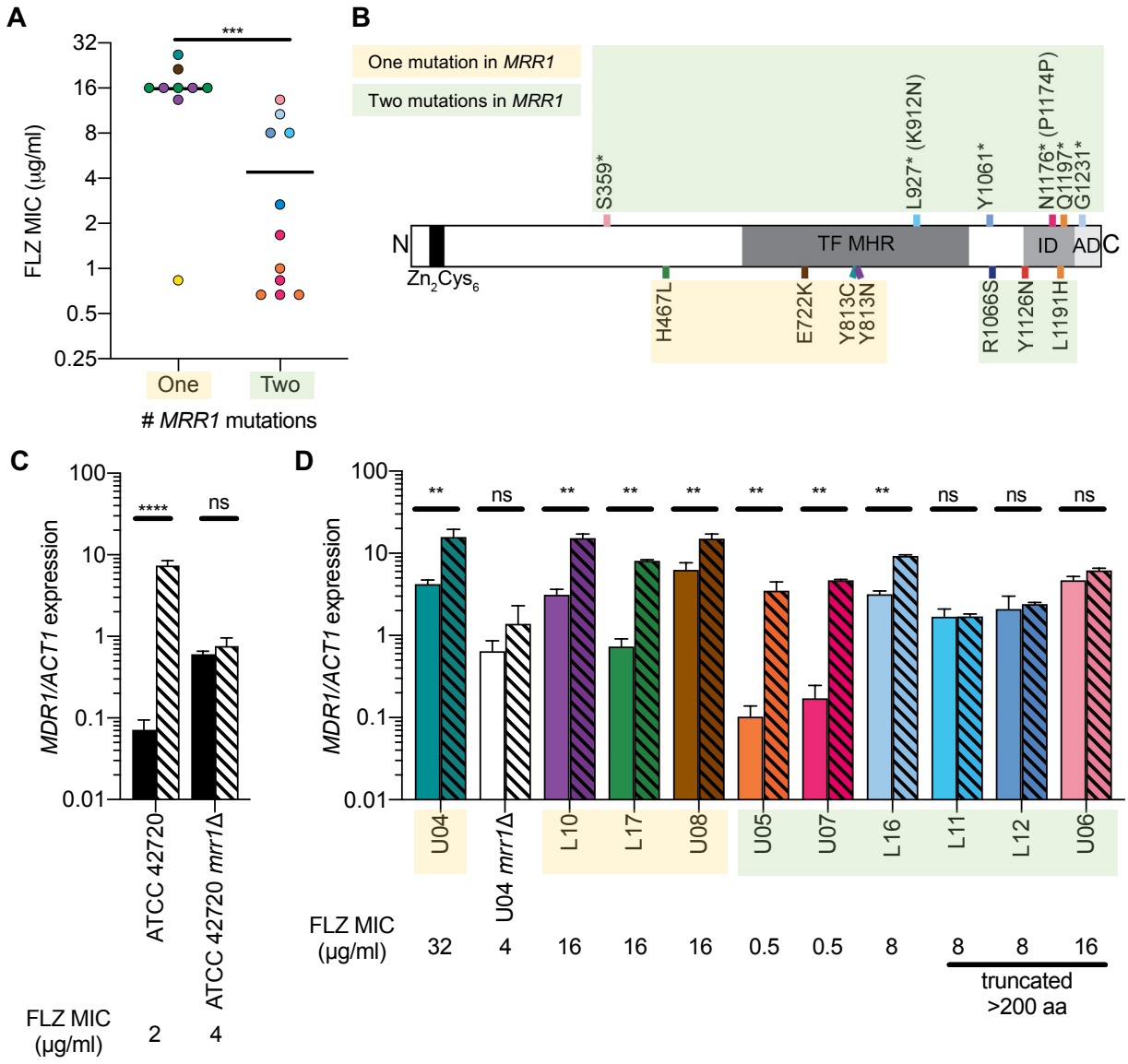

607

608 **Fig. 2: Premature stop codons in Mrr1 differentially impact *MDR1* induction by benomyl.**

609 **A**, Mean FLZ MIC for each of the twenty clinical *C. lusitaniae* isolates in Fig. 1A separated by

610 the number of nonsynonymous mutations within *MRR1* (10); datapoints colored to match Fig. 1A,

611 2B and 2D. Mean of each group shown. Two-tailed unpaired t-test of $\log_2$ transformed MIC values;

612 ***, $P<0.001$. **B**, Schematic of *C. lusitaniae MRR1* annotated with putative regulatory domains

613 determined by sequence analysis or homology to *C. albicans* (22) and locations of truncating

614 (above) and activating (below) mutations, colored to match Fig. 1A, 2A and 2D. Putative domains

include the DNA binding domain with a zinc cluster motif (Zn_2Cys_6; amino acids 33 to 61), the transcriptional regulatory middle homology region (MHR; amino acids ~607-1023), an inhibitory domain (ID; amino acids 1123 to 1217) and an activating domain (AD; amino acids 1218 to 1265). L927 and N1176 are the locations of stop codons caused by indels in codons K912 and P1174, respectively. **C** and **D**, *MDR1* expression normalized to *ACT1* in the absence (solid) or presence (striped) of 50 μg/ml benomyl. Mean ± SD of representative data in biological triplicate shown, similar trends observed on at least three different days. In **D**, Bars are colored to correspond to Fig. 1A, and strains names are highlighted to correspond to the number of nonsynonymous SNPs in *MRR1*, yellow for one and green for two. **C** and **D**, Two-way ANOVA with Sidak's multiple comparisons test; **, $P<0.0$; ****, $P<0.0001$; ns, not significant.

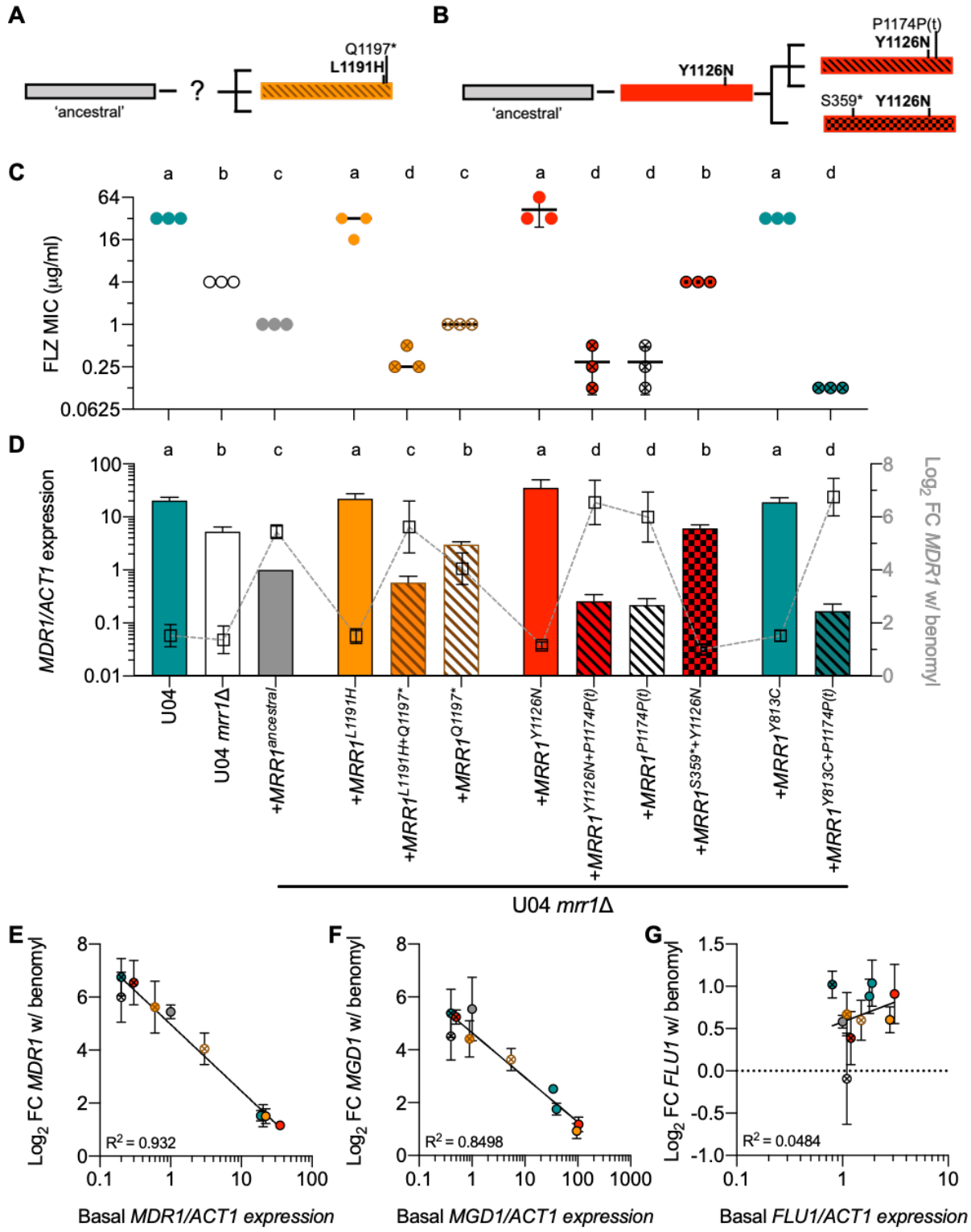

626

627 **Fig. 3: Premature stop codons repeatedly arose in constitutively active Mrr1 variants**

628 **resulting in reduced basal Mrr1 activity, but in some cases restored Mrr1 inducibility. A** and

629 **B**, Schematic of inferred evolution of *MRR1* alleles in the L1191H+Q1197* (**A**) and Y1126N (**B**)
630 lineages. **C**, FLZ MIC for U04, U04 *mrr1*Δ and *MRR1* complemented strains in the U04 *mrr1*Δ
631 background, denoted by allele. Mean ± SD of three independent assays on different days shown.
632 One-way ANOVA with Tukey's multiple comparisons test of $\log_2$ transformed values; all pairwise
633 comparisons, $P<0.01$. **D**, *MDR1* expression normalized to *ACT1* from culture grown in YPD (bars,
634 left y-axis). Mean ± SD of three independent assays on different days; data from each day was
635 normalized to the expression of U04 *mrr1*Δ +*MRR1*^{ancestral}. One-way ANOVA with Tukey's
636 multiple comparisons testing of $\log_2$ transformed data; b-d, $P<0.05$; all other pairwise
637 comparisons, $P<0.01$. Overlaid with $\log_2$ mean ± SD fold change in normalized *MDR1* expression
638 following exposure to 50 μg/ml benomyl (squares, right y-axis); full data presented with statistics
639 in Fig. S3D. **C** and **D**, FLZ MIC and *MDR1*/*ACT1* expression data are colored to match; the sample
640 names are shown on the x-axis of Fig. 3D. **E-G**, Comparison of mean basal *MDR1* (**E**), *MGD1* (**F**)
641 or *FLU1* (**G**) expression from Fig. 3D, S3B or S3C, excluding strains lacking functional *MRR1*,
642 and mean ± SD $\log_2$ fold change (FC) induction following benomyl exposure from Fig. S3D-F.
643 Goodness of fit r squared value for nonlinear regression shown.
644

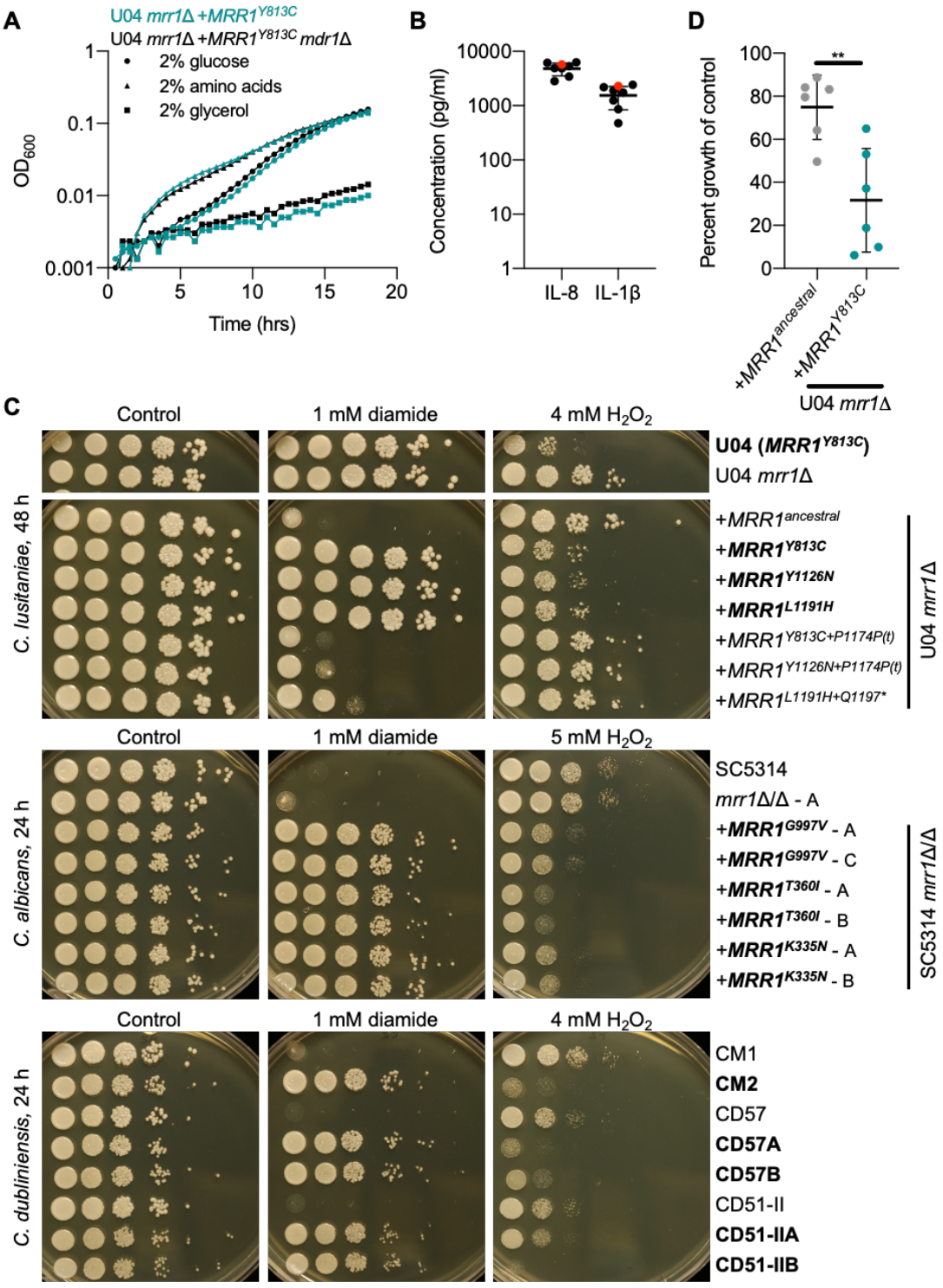

645

646 **Figure 4: Tradeoff between constitutive Mrr1 activity conferring increased resistance to**

647 **diamide but decreased resistance to hydrogen peroxide. A**, Growth curve of U04 *mrr1*Δ

+*MRR1*^{Y813C} (teal) and U04 *mrr1*Δ +*MRR1*^{Y813C} *mdr1*Δ (black) grown in YNB medium supplemented with the indicated carbon source: glucose (circles), amino acids (triangles), or glycerol (squares). Mean ± SD of representative data shown; grown at 37 °C. **B**, Quantification of cytokines IL-8 and IL-1β in BAL fluid from the CF patient with (red) or seven patients without (black) *C. lusitaniae* in their lungs. Two-way ANOVA with Sidak's multiple comparisons testing found no significant differences. **C**, Serial dilution assays of *C. lusitaniae*, *C. albicans* and *C. dubliniensis strains* on YPD or YPD supplemented with the indicated concentration of diamide or H_2O_2. Strain names in bold have been shown in to contain GOF mutations in Mrr1 resulting in increased FLZ resistance (Fig. 3C and (40, 46, 47)). Plates were imaged after 24- or 48-hours growth at 37 ºC, as indicated. **D**, Percent growth in well aerated 5 ml YPD + 1 mM H_2O_2 was calculated relative to the vehicle only control, after 22-24 hours growth at 37 ºC. These data represent six independent assays performed on different days. Significance determined by paired t-test; $^{**}P<0.01$.

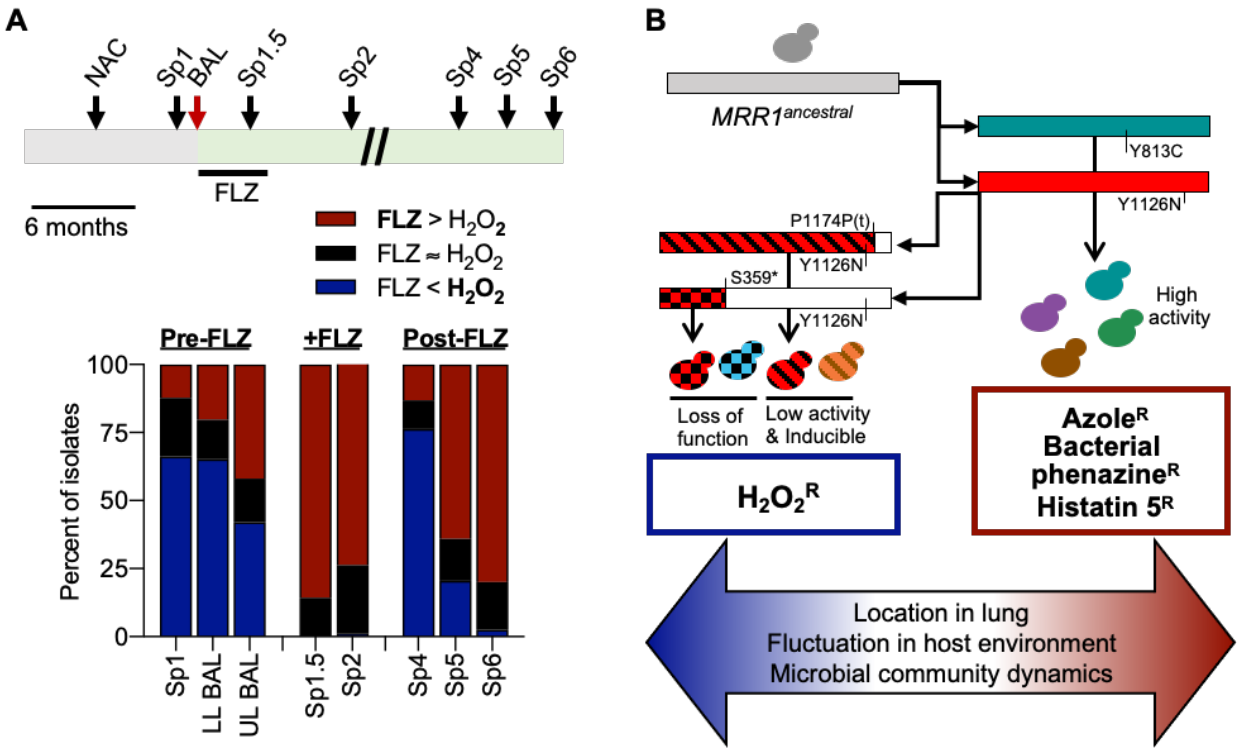

662

663 **Fig. 5: Tradeoff between FLZ and H_2O_2 resistance persists in evolving *C. lusitaniae***

664 **populations during a chronic lung infection. A**, Schematic of sampling timeline (top) and

665 histogram of the number of isolates that i) were mostly uninhibited on FLZ, but were inhibited

666 by H_2O_2 (red), ii) were mostly uninhibited on H_2O_2 but were inhibited by FLZ (blue), or iii) grew

667 similarly in both conditions (black). For the schematic, the gray bar represents the 6-10 months

668 before the BAL during which this patient was identified as being colonized by non-*albicans*

669 *Candida* (NAC) species. *C. lusitaniae* was determined to be the dominate microbe in the upper

670 and lower lobe (UL and LL, respectively) BAL samples, which marks the start of the green bar.

671 Sp1 was obtained one month before the BAL and was retrospectively also found to contain

672 abundant *C. lusitaniae*. Sp1.5, Sp2, Sp4, Sp5 and Sp6 were obtained three, nine, thirty-two,

673 thirty-five and thirty-eight months, respectively, after the BAL and all contained *C. lusitaniae*. A

674 four-month course of FLZ therapy was given after the BAL. Scale of schematic is 1 inch = 6

675 months. Multiple isolates were collected from each sample/timepoint and assayed for growth on
676 YPD supplemented with 8 μg/ml FLZ or 4 mM H_2O_2 after 48 hours at 37 ºC. Growth was scored
677 as completely inhibited, partially inhibited or uninhibited compared to a YPD only control. **B**,
678 Model for the evolution of *C. lusitaniae MRR1* in this population. Whole genome sequencing
679 and mutation analyses have shown that following the initial infection with *C. lusitaniae* encoding
680 the Mrr1-ancestral variant, a combination of exposure to different stimuli that changed overtime
681 or by locations within the CF lung environment lead to the selection for multiple constitutively
682 active Mrr1 variants, some of which persisted over time and others that were subsequently
683 mutated again resulting in premature stop codons that resulted in reversion to low activity that
684 was inducible or complete loss of Mrr1 activity. The balance between selective pressures
685 resulted in a heterogeneous population of isolates with varying resistance to biologically and
686 clinically important compounds.

687

688 **Acknowledgments**

689 We would like to thank J. Morschhäuser (Universität Würzburg) and L. Myers (Dartmouth
690 College) for sharing *C. albicans* and *C. dubliniensis* strains. Research reported in this publication
691 was supported by National Institute of Health (NIH) grant R01 AI127548 to D.A.H. from the
692 National Institute of Allergy and Infectious Disease, R01 HL122372 to A.A. from the National
693 Heart, Lung and Blood Institute, and National Institute of General Medical Sciences (NIGMS) of
694 the NIH under award number T32GM008704 and AI133956 to E.G.D. J.E.S. is a CIFAR Fellow
695 in the program Fungal Kingdom: Threats and Opportunities. This work was also supported by the
696 Cystic Fibrosis Foundation Research Development Program (CFFRDP) STANTO19R0 for the
697 Translational Research Core, and ASHARE20P0 to A.A. Sequencing services and specialized
698 equipment was provided by the Genomics and Molecular Biology Shared Resource Core at
699 Dartmouth, and Luminex analysis was performed by the DartLab – Immune Monitoring and Flow
700 Cytometry Resource Core at Dartmouth, both supported by NCI Cancer Center Support Grant
701 5P30CA023108-37. Equipment used was supported by the NIH IDeA award to Dartmouth BioMT
702 P20-GM113132. Analyses were performed using the computational and data storage resources of
703 the University of California-Riverside HPCC funded by grants from the National Science
704 Foundation (NSF) (MRI-1429826) and NIH (1S10OD016290-01A1). The content is solely the
705 responsibility of the authors and does not necessarily represent the official views of the NIH.
706

References

1. Morley VJ, Woods RJ, Read AF. 2019. Bystander selection for antimicrobial resistance: Implications for patient health. Trends Microbiol 27:864-877.
2. Holmes AH, Moore LS, Sundsfjord A, Steinbakk M, Regmi S, Karkey A, Guerin PJ, Piddock LJ. 2016. Understanding the mechanisms and drivers of antimicrobial resistance. Lancet 387:176-87.
3. Iwu CD, Korsten L, Okoh AI. 2020. The incidence of antibiotic resistance within and beyond the agricultural ecosystem: A concern for public health. Microbiologyopen doi:10.1002/mbo3.1035:e1035.
4. Pisoschi AM, Pop A, Georgescu C, Turcus V, Olah NK, Mathe E. 2018. An overview of natural antimicrobials role in food. Eur J Med Chem 143:922-935.
5. Challinor VL, Bode HB. 2015. Bioactive natural products from novel microbial sources. Ann N Y Acad Sci 1354:82-97.
6. Lieberman TD, Michel JB, Aingaran M, Potter-Bynoe G, Roux D, Davis MR, Jr., Skurnik D, Leiby N, LiPuma JJ, Goldberg JB, McAdam AJ, Priebe GP, Kishony R. 2011. Parallel bacterial evolution within multiple patients identifies candidate pathogenicity genes. Nat Genet 43:1275-80.
7. Winstanley C, O'Brien S, Brockhurst MA. 2016. *Pseudomonas aeruginosa* Evolutionary Adaptation and Diversification in Cystic Fibrosis Chronic Lung Infections. Trends Microbiol 24:327-37.
8. Lieberman TD, Flett KB, Yelin I, Martin TR, McAdam AJ, Priebe GP, Kishony R. 2014. Genetic variation of a bacterial pathogen within individuals with cystic fibrosis provides a record of selective pressures. Nat Genet 46:82-7.
9. Ciofu O, Lee B, Johannesson M, Hermansen NO, Meyer P, Hoiby N. 2008. Investigation of the algT operon sequence in mucoid and non-mucoid *Pseudomonas aeruginosa* isolates from 115 Scandinavian patients with cystic fibrosis and in 88 in vitro non-mucoid revertants. Microbiology (Reading) 154:103-113.
10. Demers EG, Biermann AR, Masonjones S, Crocker AW, Ashare A, Stajich JE, Hogan DA. 2018. Evolution of drug resistance in an antifungal-naive chronic *Candida lusitaniae* infection. Proc Natl Acad Sci U S A 115:12040-12045.
11. Chen SC, Marriott D, Playford EG, Nguyen Q, Ellis D, Meyer W, Sorrell TC, Slavin M, Australian Candidaemia S. 2009. Candidaemia with uncommon *Candida* species: predisposing factors, outcome, antifungal susceptibility, and implications for management. Clin Microbiol Infect 15:662-9.
12. Favel A, Michel-Nguyen A, Peyron F, Martin C, Thomachot L, Datry A, Bouchara JP, Challier S, Noel T, Chastin C, Regli P. 2003. Colony morphology switching of *Candida lusitaniae* and acquisition of multidrug resistance during treatment of a renal infection in a newborn: case report and review of the literature. Diagn Microbiol Infect Dis 47:331-9.
13. Kannan A, Asner SA, Trachsel E, Kelly S, Parker J, Sanglard D. 2019. Comparative Genomics for the Elucidation of Multidrug Resistance in *Candida lusitaniae*. mBio 10.
14. Asner SA, Giulieri S, Diezi M, Marchetti O, Sanglard D. 2015. Acquired multidrug antifungal resistance in *Candida lusitaniae* during therapy. Antimicrob Agents Chemother 59:7715-22.

15. Olm MR, West PT, Brooks B, Firek BA, Baker R, Morowitz MJ, Banfield JF. 2019. Genome-resolved metagenomics of eukaryotic populations during early colonization of premature infants and in hospital rooms. Microbiome 7:26.
16. Desnos-Ollivier M, Moquet O, Chouaki T, Guerin AM, Dromer F. 2011. Development of echinocandin resistance in *Clavispora lusitaniae* during caspofungin treatment. J Clin Microbiol 49:2304-6.
17. Hawkins JL, Baddour LM. 2003. *Candida lusitaniae* infections in the era of fluconazole availability. Clin Infect Dis 36:e14-8.
18. Atkinson BJ, Lewis RE, Kontoyiannis DP. 2008. *Candida lusitaniae* fungemia in cancer patients: risk factors for amphotericin B failure and outcome. Med Mycol 46:541-6.
19. Reboutier D, Piednoel M, Boisnard S, Conti A, Chevalier V, Florent M, Gibot-Leclerc S, Da Silva B, Chastin C, Fallague K, Favel A, Noel T, Ruprich-Robert G, Chapeland-Leclerc F, Papon N. 2009. Combination of different molecular mechanisms leading to fluconazole resistance in a *Candida lusitaniae* clinical isolate. Diagn Microbiol Infect Dis 63:188-93.
20. Shen XX, Zhou X, Kominek J, Kurtzman CP, Hittinger CT, Rokas A. 2016. Reconstructing the backbone of the *Saccharomycotina* yeast phylogeny using genome-scale data. G3 (Bethesda) 6:3927-3939.
21. Brown JL, Delaney C, Short B, Butcher MC, McKloud E, Williams C, Kean R, Ramage G. 2020. *Candida auris* phenotypic heterogeneity determines pathogenicity *in vitro*. mSphere 5.
22. Chow NA, Munoz JF, Gade L, Berkow EL, Li X, Welsh RM, Forsberg K, Lockhart SR, Adam R, Alanio A, Alastruey-Izquierdo A, Althawadi S, Arauz AB, Ben-Ami R, Bharat A, Calvo B, Desnos-Ollivier M, Escandon P, Gardam D, Gunturu R, Heath CH, Kurzai O, Martin R, Litvintseva AP, Cuomo CA. 2020. Tracing the Evolutionary History and Global Expansion of Candida auris Using Population Genomic Analyses. mBio 11.
23. Cuomo CA, Alanio A. 2020. Tracking a global threat: a new genotyping method for *Candida auris*. mBio 11.
24. Du H, Bing J, Hu T, Ennis CL, Nobile CJ, Huang G. 2020. *Candida auris*: Epidemiology, biology, antifungal resistance, and virulence. PLoS Pathog 16:e1008921.
25. Kean R, Brown J, Gulmez D, Ware A, Ramage G. 2020. *Candida auris*: A decade of understanding of an enigmatic pathogenic yeast. J Fungi (Basel) 6.
26. Munoz JF, Gade L, Chow NA, Loparev VN, Juieng P, Berkow EL, Farrer RA, Litvintseva AP, Cuomo CA. 2018. Genomic insights into multidrug-resistance, mating and virulence in *Candida auris* and related emerging species. Nat Commun 9:5346.
27. Zhang L, Xiao M, Watts MR, Wang H, Fan X, Kong F, Xu YC. 2015. Development of fluconazole resistance in a series of *Candida parapsilosis* isolates from a persistent candidemia patient with prolonged antifungal therapy. BMC Infect Dis 15:340.
28. Franz R, Kelly SL, Lamb DC, Kelly DE, Ruhnke M, Morschhauser J. 1998. Multiple molecular mechanisms contribute to a stepwise development of fluconazole resistance in clinical *Candida albicans* strains. Antimicrob Agents Chemother 42:3065-72.
29. Morschhauser J, Barker KS, Liu TT, Bla BWJ, Homayouni R, Rogers PD. 2007. The transcription factor Mrr1p controls expression of the *MDR1* efflux pump and mediates multidrug resistance in *Candida albicans*. PLoS Pathog 3:e164.
30. Schubert S, Rogers PD, Morschhauser J. 2008. Gain-of-function mutations in the transcription factor *MRR1* are responsible for overexpression of the *MDR1* efflux pump in fluconazole-resistant *Candida dubliniensis* strains. Antimicrob Agents Chemother 52:4274-80.

795 31. Dunkel N, Blass J, Rogers PD, Morschhauser J. 2008. Mutations in the multi-drug
796 resistance regulator *MRR1*, followed by loss of heterozygosity, are the main cause of *MDR1*
797 overexpression in fluconazole-resistant *Candida albicans* strains. Mol Microbiol 69:827-40.
798 32. Branco J, Silva AP, Silva RM, Silva-Dias A, Pina-Vaz C, Butler G, Rodrigues AG,
799 Miranda IM. 2015. Fluconazole and voriconazole resistance in *Candida parapsilosis* is conferred
800 by gain-of-function mutations in *MRR1* transcription factor gene. Antimicrob Agents Chemother
801 59:6629-33.
802 33. Biermann AR, Demers EG, Hogan DA. 2020. Mrr1 regulation of methylglyoxal
803 catabolism and methylglyoxal-induced fluconazole resistance in *Candida lusitaniae*. bioRxiv
804 doi:10.1101/2020.05.18.101840.
805 34. Krugel H, Fiedler G, Haupt I, Sarfert E, Simon H. 1988. Analysis of the nourseothricin-
806 resistance gene (nat) of *Streptomyces noursei*. Gene 62:209-17.
807 35. Staib P, Moran GP, Sullivan DJ, Coleman DC, Morschhauser J. 2001. Isogenic strain
808 construction and gene targeting in *Candida dubliniensis*. J Bacteriol 183:2859-65.
809 36. Karababa M, Coste AT, Rognon B, Bille J, Sanglard D. 2004. Comparison of gene
810 expression profiles of *Candida albicans* azole-resistant clinical isolates and laboratory strains
811 exposed to drugs inducing multidrug transporters. Antimicrob Agents Chemother 48:3064-79.
812 37. Harry JB, Oliver BG, Song JL, Silver PM, Little JT, Choiniere J, White TC. 2005. Drug-
813 induced regulation of the *MDR1* promoter in *Candida albicans*. Antimicrob Agents Chemother
814 49:2785-92.
815 38. Kwak MK, Ku M, Kang SO. 2018. Inducible NAD(H)-linked methylglyoxal
816 oxidoreductase regulates cellular methylglyoxal and pyruvate through enhanced activities of
817 alcohol dehydrogenase and methylglyoxal-oxidizing enzymes in glutathione-depleted *Candida*
818 *albicans*. Biochim Biophys Acta Gen Subj 1862:18-39.
819 39. Calabrese D, Bille J, Sanglard D. 2000. A novel multidrug efflux transporter gene of the
820 major facilitator superfamily from *Candida albicans* (*FLU1*) conferring resistance to
821 fluconazole. Microbiology 146 (Pt 11):2743-54.
822 40. Hampe IAI, Friedman J, Edgerton M, Morschhauser J. 2017. An acquired mechanism of
823 antifungal drug resistance simultaneously enables *Candida albicans* to escape from intrinsic host
824 defenses. PLoS Pathog 13:e1006655.
825 41. Alonso A, Martinez JL. 2001. Expression of multidrug efflux pump SmeDEF by clinical
826 isolates of *Stenotrophomonas maltophilia*. Antimicrob Agents Chemother 45:1879-81.
827 42. Praski Alzrigat L, Huseby DL, Brandis G, Hughes D. 2017. Fitness cost constrains the
828 spectrum of marR mutations in ciprofloxacin-resistant *Escherichia coli*. J Antimicrob Chemother
829 72:3016-3024.
830 43. Popp C, Hampe IAI, Hertlein T, Ohlsen K, Rogers PD, Morschhauser J. 2017.
831 Competitive fitness of fluconazole-resistant clinical *Candida albicans* strains. Antimicrob
832 Agents Chemother 61.
833 44. Rottner M, Freyssinet JM, Martinez MC. 2009. Mechanisms of the noxious inflammatory
834 cycle in cystic fibrosis. Respir Res 10:23.
835 45. Laval J, Ralhan A, Hartl D. 2016. Neutrophils in cystic fibrosis. Biol Chem 397:485-96.
836 46. Moran GP, Sanglard D, Donnelly SM, Shanley DB, Sullivan DJ, Coleman DC. 1998.
837 Identification and expression of multidrug transporters responsible for fluconazole resistance in
838 *Candida dubliniensis*. Antimicrob Agents Chemother 42:1819-30.
839 47. Moran GP, Sullivan DJ, Henman MC, McCreary CE, Harrington BJ, Shanley DB,
840 Coleman DC. 1997. Antifungal drug susceptibilities of oral *Candida dubliniensis* isolates from

841 human immunodeficiency virus (HIV)-infected and non-HIV-infected subjects and generation of
842 stable fluconazole-resistant derivatives *in vitro*. Antimicrob Agents Chemother 41:617-23.
843 48. da Silva AR, de Andrade Neto JB, da Silva CR, Campos Rde S, Costa Silva RA, Freitas
844 DD, do Nascimento FB, de Andrade LN, Sampaio LS, Grangeiro TB, Magalhaes HI, Cavalcanti
845 BC, de Moraes MO, Nobre Junior HV. 2016. Berberine antifungal activity in fluconazole-
846 resistant pathogenic yeasts: Action mechanism evaluated by flow cytometry and biofilm growth
847 inhibition in *Candida* spp. Antimicrob Agents Chemother 60:3551-7.
848 49. Wakiec R, Gabriel I, Prasad R, Becker JM, Payne JW, Milewski S. 2008. Enhanced
849 susceptibility to antifungal oligopeptides in yeast strains overexpressing ABC multidrug efflux
850 pumps. Antimicrob Agents Chemother 52:4057-63.
851 50. Liu S, Yue L, Gu W, Li X, Zhang L, Sun S. 2016. Synergistic effect of fluconazole and
852 calcium channel blockers against resistant *Candida albicans*. PLoS One 11:e0150859.
853 51. Kaur R, Castano I, Cormack BP. 2004. Functional genomic analysis of fluconazole
854 susceptibility in the pathogenic yeast *Candida glabrata*: roles of calcium signaling and
855 mitochondria. Antimicrob Agents Chemother 48:1600-13.
856 52. Ludewig G, Williams JM, Li Y, Staben C. 1994. Effects of pentamidine isethionate on
857 *Saccharomyces cerevisiae*. Antimicrob Agents Chemother 38:1123-8.
858 53. Cox LJ, Dooley D, Beumer R. 1990. Effect of lithium chloride and other inhibitors on the
859 growth of *Listeria* spp. Food Microbiology 7:311-325.
860 54. Xu Y, Wang Y, Yan L, Liang RM, Dai BD, Tang RJ, Gao PH, Jiang YY. 2009.
861 Proteomic analysis reveals a synergistic mechanism of fluconazole and berberine against
862 fluconazole-resistant *Candida albicans*: endogenous ROS augmentation. J Proteome Res 8:5296-
863 304.
864 55. Dhamgaye S, Devaux F, Vandeputte P, Khandelwal NK, Sanglard D, Mukhopadhyay G,
865 Prasad R. 2014. Molecular mechanisms of action of herbal antifungal alkaloid berberine, in
866 *Candida albicans*. PLoS One 9:e104554.
867 56. Henderson G. 1989. A comparison of the effects of chromate, molybdate and cadmium
868 oxide on respiration in the yeast *Saccharomyces cerevisiae*. Biol Met 2:83-8.
869 57. Edwards KJ, Jenkins TC, Neidle S. 1992. Crystal structure of a pentamidine-
870 oligonucleotide complex: implications for DNA-binding properties. Biochemistry 31:7104-9.
871 58. Lerman LS. 1961. Structural considerations in the interaction of DNA and acridines. J
872 Mol Biol 3:18-30.
873 59. Krey AK, Hahn FE. 1969. Berberine: complex with DNA. Science 166:755-7.
874 60. Exinger F, Lacroute F. 1992. 6-Azauracil inhibition of GTP biosynthesis in
875 *Saccharomyces cerevisiae*. Curr Genet 22:9-11.
876 61. Handschumacher RE. 1960. Orotidylic acid decarboxylase: inhibition studies with
877 azauridine 5'-phosphate. J Biol Chem 235:2917-9.
878 62. Bridgewater LC, Manning FC, Patierno SR. 1994. Base-specific arrest of *in vitro* DNA
879 replication by carcinogenic chromium: relationship to DNA interstrand crosslinking.
880 Carcinogenesis 15:2421-7.
881 63. Grahl N, Demers EG, Crocker AW, Hogan DA. 2017. Use of RNA-protein complexes
882 for genome editing in non-*albicans Candida* species. mSphere 2.
883 64. Schubert S, Barker KS, Znaidi S, Schneider S, Dierolf F, Dunkel N, Aid M, Boucher G,
884 Rogers PD, Raymond M, Morschhauser J. 2011. Regulation of efflux pump expression and drug
885 resistance by the transcription factors Mrr1, Upc2, and Cap1 in *Candida albicans*. Antimicrob
886 Agents Chemother 55:2212-23.

887 65. Enjalbert B, Nantel A, Whiteway M. 2003. Stress-induced gene expression in *Candida*
888 *albicans*: absence of a general stress response. Mol Biol Cell 14:1460-7.
889 66. Enjalbert B, Smith DA, Cornell MJ, Alam I, Nicholls S, Brown AJ, Quinn J. 2006. Role
890 of the Hog1 stress-activated protein kinase in the global transcriptional response to stress in the
891 fungal pathogen *Candida albicans*. Mol Biol Cell 17:1018-32.
892 67. Arastehfar A, Daneshnia F, Hilmioglu-Polat S, Fang W, Yasar M, Polat F, Metin DY,
893 Rigole P, Coenye T, Ilkit M, Pan W, Liao W, Hagen F, Kostrzewa M, Perlin DS, Lass-Florl C,
894 Boekhout T. 2020. First report of candidemia clonal outbreak caused by emerging fluconazole-
895 resistant *Candida parapsilosis* isolates harboring Y132F and/or Y132F+K143R in Turkey.
896 Antimicrob Agents Chemother 64.
897 68. Schubert S, Popp C, Rogers PD, Morschhauser J. 2011. Functional dissection of a
898 *Candida albicans* zinc cluster transcription factor, the multidrug resistance regulator Mrr1.
899 Eukaryot Cell 10:1110-21.
900 69. Liu Z, Myers LC. 2017. *Candida albicans* Swi/Snf and Mediator Complexes
901 Differentially Regulate Mrr1-Induced *MDR1* Expression and Fluconazole Resistance.
902 Antimicrob Agents Chemother 61.
903 70. Mogavero S, Tavanti A, Senesi S, Rogers PD, Morschhauser J. 2011. Differential
904 requirement of the transcription factor Mcm1 for activation of the *Candida albicans* multidrug
905 efflux pump *MDR1* by its regulators Mrr1 and Cap1. Antimicrob Agents Chemother 55:2061-6.
906 71. Hull J, Vervaart P, Grimwood K, Phelan P. 1997. Pulmonary oxidative stress response in
907 young children with cystic fibrosis. Thorax 52:557-60.
908 72. Brown RK, Kelly FJ. 1994. Evidence for increased oxidative damage in patients with
909 cystic fibrosis. Pediatr Res 36:487-93.
910 73. Warris A, Ballou ER. 2019. Oxidative responses and fungal infection biology. Semin
911 Cell Dev Biol 89:34-46.
912 74. Hogan DA, Willger SD, Dolben EL, Hampton TH, Stanton BA, Morrison HG, Sogin
913 ML, Czum J, Ashare A. 2016. Analysis of lung microbiota in bronchoalveolar lavage, protected
914 brush and sputum samples from subjects with mild-to-moderate cystic fibrosis lung disease.
915 PLoS One 11:e0149998.
916 75. Min K, Ichikawa Y, Woolford CA, Mitchell AP. 2016. *Candida albicans* gene deletion
917 with a transient CRISPR-Cas9 system. mSphere 1.
918 76. Basso LR, Jr., Bartiss A, Mao Y, Gast CE, Coelho PS, Snyder M, Wong B. 2010.
919 Transformation of Candida albicans with a synthetic hygromycin B resistance gene. Yeast
920 27:1039-48.
921 77. Christianson TW, Sikorski RS, Dante M, Shero JH, Hieter P. 1992. Multifunctional yeast
922 high-copy-number shuttle vectors. Gene 110:119-22.
923 78. Shanks RM, Caiazza NC, Hinsa SM, Toutain CM, O'Toole GA. 2006. *Saccharomyces*
924 *cerevisiae*-based molecular tool kit for manipulation of genes from gram-negative bacteria. Appl
925 Environ Microbiol 72:5027-36.
926 79. Butler G, Rasmussen MD, Lin MF, Santos MA, Sakthikumar S, Munro CA, Rheinbay E,
927 Grabherr M, Forche A, Reedy JL, Agrafioti I, Arnaud MB, Bates S, Brown AJ, Brunke S,
928 Costanzo MC, Fitzpatrick DA, de Groot PW, Harris D, Hoyer LL, Hube B, Klis FM, Kodira C,
929 Lennard N, Logue ME, Martin R, Neiman AM, Nikolaou E, Quail MA, Quinn J, Santos MC,
930 Schmitzberger FF, Sherlock G, Shah P, Silverstein KA, Skrzypek MS, Soll D, Staggs R,
931 Stansfield I, Stumpf MP, Sudbery PE, Srikantha T, Zeng Q, Berman J, Berriman M, Heitman J,

932 Gow NA, Lorenz MC, Birren BW, Kellis M, et al. 2009. Evolution of pathogenicity and sexual
933 reproduction in eight *Candida* genomes. Nature 459:657-62.
934 80. CLSI. 2012. Reference method for broth dilution antifungal susceptibility testing of
935 yeasts, vol CLSI document M27-S4. Wayne: Clinical and Laboratory Standard Institute.
936 81. Wu TD, Reeder J, Lawrence M, Becker G, Brauer MJ. 2016. GMAP and GSNAP for
937 Genomic Sequence Alignment: Enhancements to Speed, Accuracy, and Functionality. Methods
938 Mol Biol 1418:283-334.
939 82. Liao Y, Smyth GK, Shi W. 2014. featureCounts: an efficient general purpose program for
940 assigning sequence reads to genomic features. Bioinformatics 30:923-30.
941 83. Robinson MD, McCarthy DJ, Smyth GK. 2010. edgeR: a Bioconductor package for
942 differential expression analysis of digital gene expression data. Bioinformatics 26:139-40.
943

944